Supplement of Atmos. Chem. Phys., 15, 9983–9996, 2015
http://www.atmos-chem-phys.net/15/9983/2015/
doi:10.5194/acp-15-9983-2015-supplement

Supplement of

Diesel-related hydrocarbons can dominate gas phase reactive carbon in megacities

R. E. Dunmore et al.

Correspondence to: J. Hamilton (jacqui.hamilton@york.ac.uk)

1 Supplementary Information

1.1 Speciated Emission Inventory Calculations

The speciated emissions inventory supplied in a report from Passant (2002) provides data on a large range of individual NMHCs and their specific emission sources. From this comprehensive speciation profile, it is possible to apply the most recent UK National Atmospheric Emissions Inventory (NAEI) from 2012 and calculate scaling factors that can applied to each source category (The UK NAEI data is available at http://naei.defra.gov.uk/data/data-selector, and was accessed on 30/01/2014). The speciated proportion profiles of the individual NMHCs emitted from given sources should not change significantly, however the total emission from a source will as a result of changes in activity levels and the impact of regulations/abatement. The US has no equivalent NAEI speciated emission inventory. The SPECIATE database (U.S. Environmental Protection Agency (EPA)) provides detailed species profiles for a larger range of emission sources (The US EPA SPECIATE data is available at http://cfpub.epa.gov/si/speciate/, and was accessed on 20/02/2014). In order to compare directly to the UK NAEI from Passant, the SPECIATE emission profiles are used to calculate scaling factors as above. All VOC sources have been included in the inventory calculation with the exception of the Forests source category, due to the lack of chemical speciation (given as isoprene+BVOC). There is a small anthropogenic emission source of terpenoids in the inventory from fuel sources and wood product manufacture categories.

1.2 Differences between London and Previous US studies

1.2.1 Weekday versus weekend differences in diesel emissons

Previous measurements of VOCs in Bakersfield showed a lower toluene/benzene ratio (t/b) at the weekend (t/b = 1.7) compared to weekdays (t/b = 2.4) (Bahreini et al., 2012). This was used as an indicator of reduced photochemistry at the weekend as a result of changes in diesel emissions due to reductions in heavy-duty vehicles. Using this same approach, the winter campaign ratio has been calculated for weekends (t/b = 2.6) and weekdays (t/b = 2.2), the opposite of the Bakersfield study, with a higher t/b ratio at the weekend, although it should be noted that the correlation between the two species is poorer during the weekdays (R^2 = 0.73, *c.f.* weekend R^2 = 0.96). Also, no discernable differences were found between the behavior of gasoline (2,2,4-trimethyl pentane and toluene) and diesel tracers (*n*-dodecane, C_{13} aliphatics) as shown in SI Figure 1, with average diurnal profiles at the weekends shown in blue and weekdays in red. In general there are lower concentrations during the evening rush hour (16:00-19:00) of all VOCs and NO_x at the weekend, with an increase later in the evening (19:00-00:00), reflecting the increase in nighttime social activities during the weekends. However, the highest mixing ratios of most VOCs were observed on Sat 14/01/2012, as a result of low wind speeds and a low boundary layer depth. The traffic make up in London is different to US cities, with a high degree of diesel powered buses and cars. Thus the influence of reduced heavy-duty truck traffic is not observed in the ratio of diesel to gasoline VOCs.

1.2.2 Comparison of London and Los Angeles

SI Table 1 shows the differences between London and Los Angeles in terms of population density, green space and diesel fuel use to highlight the very different urban geography and traffic make up in the two cities. A smaller sub set of data is also included for North Kensington, where this study was carried out and Bakersfield, CA, the site of the CALNEX project.

This comparison is particularly important when considering the sources of BVOCs. In California, where many of the previous studies have taken place, the cities are surrounded by high BVOC emitting regions *i.e.* Blodgett Forest, Angeles National Park, Sequoia National Park and Los Padres National Park. Los Angeles itself only has around 6.7% public greenery. In contrast, London has an estimated 38% public green space and is the greenest city of its size in the World. The emission maps shown in SI Figure 2 show that current emission models do not predict a significant downwind source of BVOC to London. Therefore in summer in London, the majority of BVOCs measured are likely to be from relatively local sources.

1.3 Calibrations and Uncertainties

Gas phase calibrations were performed at regular intervals on both instruments using a standard (NPL30, National Physical Laboratory, Teddington, UK) containing 30 ozone precursor species (C_2-C_8) at 3-5 ppb levels. For the higher carbon number hydrocarbons measured on the GC×GC, a separate NPL standard was used which contained 24 species from C_5-C_{11} (including a range of aromatics). However many of the higher hydrocarbon measurements from the GC×GC-FID were ultimately based on calibrations from liquid standards introduced by splitless injection. Instrument zeros, including testing of sample lines and water removal stages, were made using high purity N_2, with further purification using an Aeronex Gatekeeper catalyst.

For those compounds not included in gas standard mixtures, a response factor (RF) was calculated from liquid injections, to allow compound concentrations to be quantified (Equation 1). This was determined as the response of a compound (i) with respect to a reference compound (ref), where $R_{ref,st}$ and $R_{i,st}$ are the responses of the reference and i compounds in the standard (or in this case from liquid mixtures, st) respectively, and $C_{ref,st}$ and $C_{i,st}$ are the corresponding concentrations (de Blas et al., 2011). The response factor can then be used in a second equation to quantify the concentrations of the compounds in air samples. This is shown in Equation 2, where X_{ref} and X_i are the concentrations of the reference and i compounds in air samples, and PA_{ref} and PA_i are the peak areas of the reference and i compounds respectively. For the grouped compounds (see Figure 2 of the main paper and SI Table 3), the *n*-alkane response has been used for quantification as FID response is assumed to be linear with carbon number (Slemr et al., 2004).

$$RF_{i\cdot ref} = \frac{R_{ref,st} \times C_{i,st}}{R_{i,st} \times C_{ref,st}} \tag{1}$$

$$[X_i] = \frac{\left(\dfrac{PA_i}{PA_{ref}}\right) \times [X_{ref}]}{RF_{i\cdot ref}} \tag{2}$$

Measurement uncertainties are described in Hopkins et al. (2003) and Lidster et al. (2011) however they are broadly dominated by the gravimetric uncertainty associated with gas standard preparation, typically 5%. Run to run reproducibility was better than 1% for light C_2-C_7 hydrocarbons (when >1 ppb) and better than 5% for higher hydrocarbons. The expanded uncertainty (k=2) for the carbon class measurements reported in this article are estimated at 6% for C_2-C_7 and 5-11% for C_8-C_{13} (depending on the specific compound).

1.4 Benzene Correlations

There were a number of species that were observed on both GC instruments (*n*-hexane, 2/3-methyl pentane, *n*-heptane, *n*-octane, 2,2,4-trimethyl pentane, isoprene, benzene, toluene, ethyl benzene, *m/p*-xylene, *o*-xylene and acetone). The agreement between both instruments for these species is good as typified by the observations of benzene shown in SI Figure 4.

1.5 GC×GC-FID full identification and concentrations

Individually identified compounds are shown in SI Figure 5 (where the numbers represent the peak identity in SI Table 2), a typical GC×GC-FID plot, where the retention times from column 1 (separation based on volatility) and column 2 (separation based on polarity) are the x and y axis respectively, and compound intensity is the coloured contour. Two simplified bands of compounds can be seen; an aromatic band that is well separated from the aliphatic band, however, these are just general features and some oxygenated and other hetero species are present: both within and outside these lines. Figure 5b and 5c are expanded sections of Figure 5a to improve visualisation.

1.6 Impact of local meteorology in winter

Ethane shows a different behaviour characteristic of a persistent fugiative release, in this case from the natural gas network (de Gouw et al., 2005; Borbon et al., 2001), and is also impacted by changing boundary layer height. In the original winter diurnal profile of ethane (which includes all data points, seen in SI Figure 6, blue profile), a pattern is seen which appears to show a large increase in the early morning hours. This is likely due to two stagnant, high pressure periods experienced at the start and end of the campaign where data profiles were driven by meteorological conditions (10/01/2012-18/01/2012 and 03/02/2012-08/02/2012). The dispersion of VOCs would be low given decreased wind speeds, and as such the ethane concentration would appear to rise.

In order to see the most accurate profile of ethane, the data points corresponding to the two stagnant periods were removed and a new diurnal profile constructed (shown in SI Figure 6, red profile). This shows the expected diurnal profile. The ‘dip’ seen in both profiles of ethane at approximately 12 noon correlates to a rise in the boundary layer. A boundary layer decrease in the afternoon is also seen to have an effect on the profiles of ethane with a small rise at approximately 15:00. There is no difference seen in the two profiles of the other individual VOCs and grouped species, except for a larger range in the unconstrained profiles, likely due to the higher concentrations seen during the two stagnant, high pressure periods and their shorter lifetime in the atmosphere compared to ethane.

1.7 Calculation of primary hydrocarbon OH reactivity

The following equation was used to calculate the primary hydrocarbon OH reactivity, using observed meteorological data (T and p). Due to a lack of information on rate constant temperature dependence for most species, the 298 K k_{OH} rate constants were used from Atkinson and Arey (2003) for all individually identified species.

$$\mathrm{s}^{-1} = \left([\mathrm{VOC}]\,(\mathrm{ppb}) \times 10^{-9} \times [\mathrm{M}]\right) \times k_{OH}\,(298\ \mathrm{K}) \tag{3}$$

Where

$$[\mathrm{M}] = \left(\frac{\mathrm{Pressure}\,(\mathrm{mbar}) \times 10^{-4}}{(8\cdot 314 \times (273\cdot 15 + \mathrm{temperature}))}\right) \times 6\cdot 022E + 23 \tag{4}$$

For each aliphatic group, the appropriate C number *n*-alkane k_{OH} rate constant was used to calculate the primary OH reactivity. Each group is likely to contain branched alkanes, cycloalkanes and alkenes in addition to the *n*-alkane. The measured rate constants of branched alkanes with OH are usually similar or slower than the linear alkane, depending on the location and degree of branching. There are very few measurements of OH rate constants for cycloalkanes, but generally they react faster than the equivalent linear alkane. Alkenes react around an order of magnitude faster with OH than alkanes, and the rate increases further with increasing degrees of unsaturation.

Due to a lack of isomer speciation and kinetic data above C_9, the *n*-alkane rate constant was used to allow direct comparison between the C_n groups. This is likely to represent a small underestimate of the group as a whole as we assume no alkene contribution to the reactivity of the group. We calculated OH rate constants (298 K) for 354 C_{12} alkane isomers using the H atom abstraction structure activity relationship defined in Ziemann and Atkinson (2012). The average rate constant was found to be 1.15×10^{-11} cm^3 $\mathrm{molecule}^{-1}$ s^{-1} which, when compared to the measured rate constant for *n*-dodecane (1.32 (± 0.26) $\times 10^{-11}$ cm^3 molecule^{-1} s^{-1}), is within the error limits for this measurement (Atkinson, 2003). A selection of the calculated rate constants are shown in SI Table 4, along with some alkenes to highlight the range of reactivities of the C_{12} species.

For the C_{10} terpenoid group the use of α-pinene rate constant (5.23 $\times 10^{-11}$ cm^3 molecule^{-1} s^{-1}) produces a conservative underestimate of the OH reactivity for this group, as it is one of the slowest reacting species, *c.f.* limonene (1.64 $\times 10^{-10}$ cm^3 molecule^{-1} s^{-1}) (Atkinson and Arey, 2003). If a rate constant half way between α-pinene and limonene (1.08 $\times 10^{-10}$ cm^3 molecule^{-1} s^{-1}) was used, this would increase the contribution of the C_{10} terpenoid group to primary OH reactivity from 0.009 s^{-1} to 0.019 s^{-1} and 0.041 s^{-1} to 0.086 s^{-1} in winter and summer respectively.

1.8 Effect of fuel composition on the calculation of emission sources

The differences in fuel composition of gasoline and diesel from the UK and US may have an effect on the calculations presented in this study. This could be particularly important for the middle range carbon number species, as the US has strict guidelines on the addition of so called “heavy hydrocarbons” (*i.e.* C_9-C_{11} aromatic species) to gasoline. By comparison, the UK has more stringent controls of the composition of diesel fuel. This has been addressed by re-calculating the contributions of total diesel emissions to mixing ratio, mass, OH reactivity and OFP with and without the specified C_9 aromatic content as presented in Gentner et al. (2013). The results of this analysis is given in SI Table 6, which shows that excepting winter OFP (2.1%), is equal to or less than a 1% difference.

1.9 Fuel usage changes

Department of Energy and Climate Change statistics (www.gov.uk/government/statistical-data-sets/road-transport-energy-consumption-at-regional-and-local-authority-level , and was accessed on 30/04/2014) give a regional breakdown of the total diesel and fuel consumption from 2005 to 2011 and are shown below for the UK in SI Table 7 and SI Figure 7.

References

Aschmann, S. and Atkinson, R.: Rate constants for the gas-phase reactions of OH radicals with *E*-7-tetradecene, 2-methyl-1-tridecene and the C_7-C_{14} 1-alkenes at 295 ± 1 K, Physical Chemistry Chemical Physics, 10, 4159–4164, doi:10.1039/B803527J, 2008.

Atkinson, R.: Kinetics of the gas-phase reactions of OH radicals with alkanes and cycloalkanes, Atmospheric Chemistry and Physics, 3, 2233–2307, doi:10.5194/acp-3-2233-2003, 2003.

Atkinson, R. and Arey, J.: Atmospheric degradation of volatile organic compounds, Chemical Reviews, 103, 4605–4638, doi:10.1021/cr0206420, 2003.

Bahreini, R., Middlebrook, A. M., de Gouw, J. A., Warneke, C., Trainer, M., Brock, C. A., Stark, H., Brown, S. S., Dube, W. P., Gilman, J. B., Hall, K., Holloway, J. S., Kuster, W. C., Perring, A. E., Prevot, A. S. H., Schwarz, J. P., Spackman, J. R., Szidat, S., Wagner, N. L., Weber, R. J., Zotter, P., and Parrish, D. D.: Gasoline emissions dominate over diesel in formation of secondary organic aerosol mass, Geophysical Research Letters, 39, doi:10.1029/2011GL050718, 2012.

Borbon, A., Fontaine, H., Veillerot, M., Locoge, N., Galloo, J., and Guillermo, R.: An investigation into the traffic-related fraction of isoprene at an urban location, Atmospheric Environment, 35, 3749–3760, doi:10.1016/S1352-2310(01)00170-4, 2001.

de Blas, M., Navazo, M., Alonso, L., Durana, N., and Iza, J.: Automatic on-line monitoring of atmospheric volatile organic compounds: Gas chromatography-mass spectrometry and gas chromatography-flame ionization detection as complementary systems, Science of the Total Environment, 409, 5459–5469, 2011.

de Gouw, J., Middlebrook, A., Warneke, C., Goldan, P., Kuster, W., Roberts, J., Fehsenfeld, F., Worsnop, D., Canagaratna, M., Pszenny, A., Keene, W., Marchewka, M., Bertman, S., and Bates, T.: Budget of organic carbon in a polluted atmosphere: Results from the New England Air Quality Study in 2002, Journal of Geophysical Research-Atmospheres, 110, doi:10.1029/2004JD005623, 2005.

Gentner, D., Isaacman, G., Worton, D., Chan, A., Dallmann, T., Davis, L., Liu, S., Day, D., Russell, L., Wilson, K., Weber, R., Guha, A., Harley, R., and Goldstein, A.: Elucidating secondary organic aerosol from diesel and gasoline vehicles through detailed characterization of organic carbon emissions, Proceedings of the National Academy of Sciences of the United States of America, 109, 18 318–23, doi:10.1073/pnas.1212272109, 2012.

Gentner, D., Worton, D., Isaacman, G., Davis, L., Dallmann, T., Wood, E., Herndon, S., Goldstein, A., and Harley, R.: Chemical composition of gas-phase organic carbon emissions from motor vehicles and implications for ozone production, Environmental Science & Technology, 47, 11 837–11 848, doi:10.1021/es401470e, 2013.

Hopkins, J., Lewis, A., and Read, K.: A two-column method for long-term monitoring of non-methane hydrocarbons (NMHCs) and oxygenated volatile organic compounds (OVOCs), Journal of Environmental Monitoring, 5, 8–13, doi:10.1039/b202798d, 2003.

Kwok, E. and Atkinson, R.: Estimation of hydroxyl radical reaction-rate constants for gas-phase organic-compounds using a struture-reactivity relathionship - an update, Atmospheric Environment, 29, 1685–1695, doi:10.1016/1352-2310(95)00069-B, 1995.

Lidster, R., Hamilton, J., and Lewis, A.: The application of two total transfer valve modulators for comprehensive two-dimensional gas chromatography of volatile organic compounds, Journal of Separation Science, 34, 812–821, doi:10.1002/jssc.201000710, 2011.

Passant, N.: Speciation of UK emissions of non-methane volatile organic compounds, Tech. rep., AEA Technology Report ENV-05452002, Culham, Abingdon, United Kingdom, 2002.

Slemr, J., Slemr, F., D'Souza, H., and Partridge, R.: Study of the relative response factors of various gas chromatograph–flame ionisation detector systems for measurement of C_2-C_9 hydrocarbons in air, Journal of Chromatography A, 1061, 75 – 84, doi:10.1016/j.chroma.2004.10.037, 2004.

Stewart, H., Hewitt, C., Bunce, R., Steinbrecher, R., Smiatek, G., and Schoenemeyer, T.: A highly spatially and temporally resolved inventory for biogenic isoprene and monoterpene emissions: Model description and application to Great Britain, Journal of Geophysical Research: Atmospheres, 108, doi:10.1029/2002JD002694, 2003.

Ziemann, P. and Atkinson, R.: Kinetics, products, and mechanisms of secondary organic aerosol formation, Chemical Society Reviews, 41, 6582–6605, doi:10.1039/C2CS35122F, 2012.

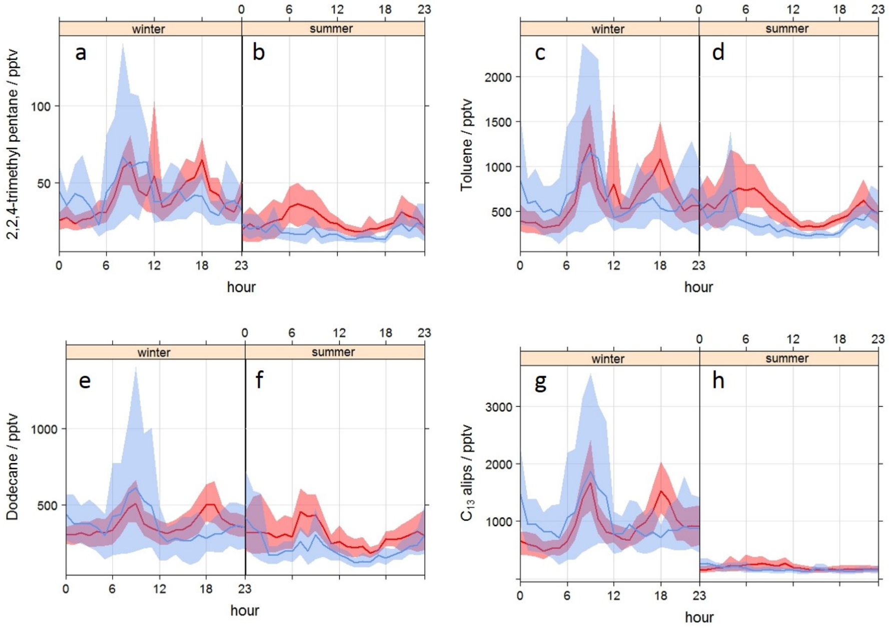

Figure 1. Diurnal profiles of typically traffic source related compounds showing weekday (red) and weekend (blue) profiles. Petrol compounds are toluene and 2,2,4-trimethyl pentane and diesel compounds are *n*-dodecane and C_{13} aliphatics

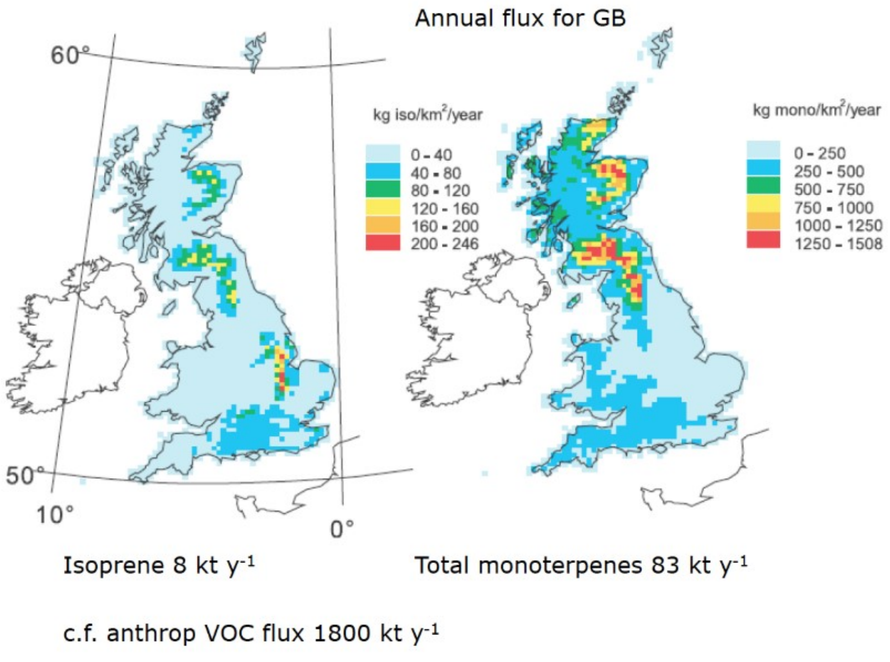

Figure 2. Isoprene and monoterpene annual flux for Great Britain in 1998. (Stewart et al., 2003)

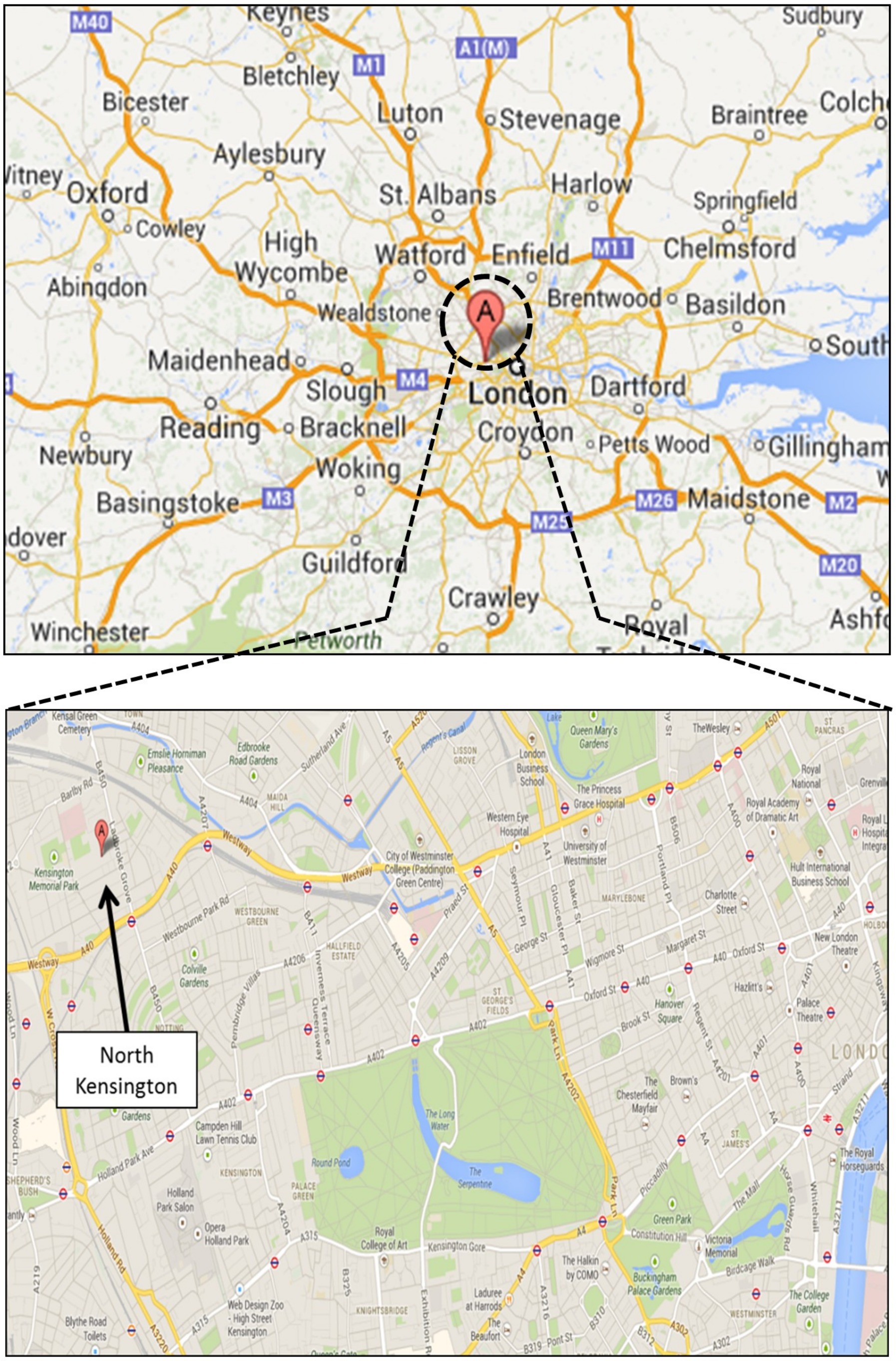

Figure 3. Location of the North Kensington site

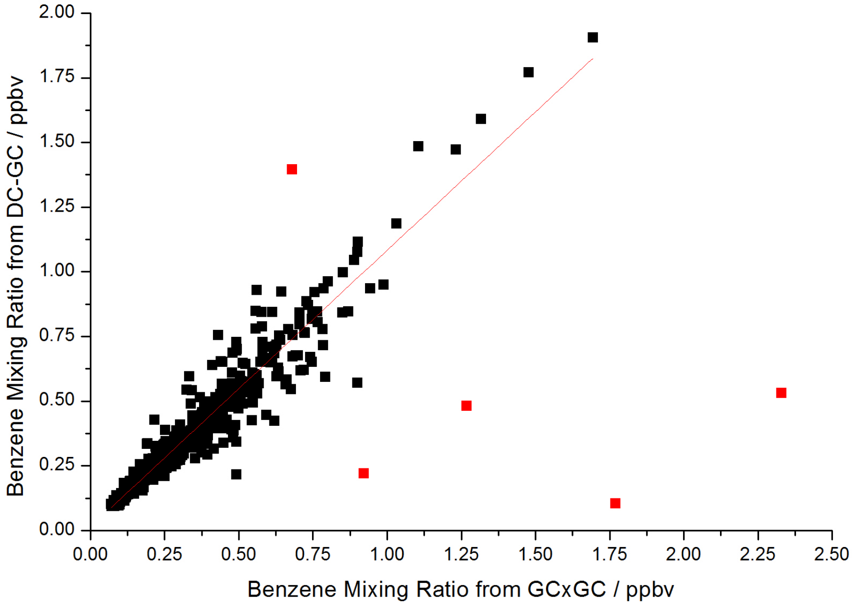

Figure 4. Benzene correlation for the GC×GC-FID (x-axis) and the DC-GC-FID (y-axis) instruments, R^2 0.92, slope 1.070 ± 0.013. Points shown in red have been removed from the correlation as outliers

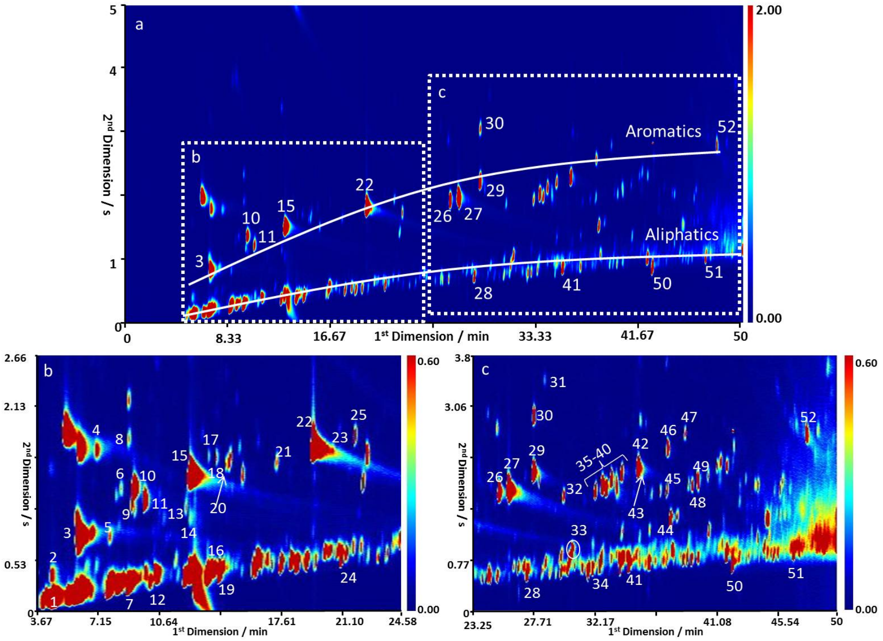

Figure 5. A typical GC×GC-FID plot from 2012-02-07 at 08:32, showing two separate bands of compounds, aromatic and aliphatics. Box b and c show zoomed in sections of the original plot. Labelled peaks for sections a, b and c are given in Table 2.

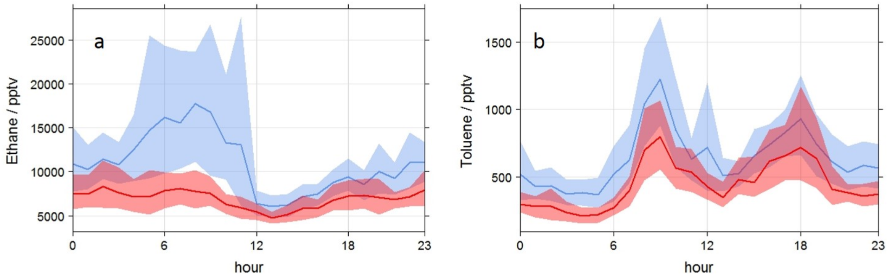

Figure 6. Winter profiles of ethane (left) and toluene (right), showing the effect of changing meteorology. a, ethane (n = 660 and 353, blue and red, respectively) and b, toluene (n = 660 and 353)

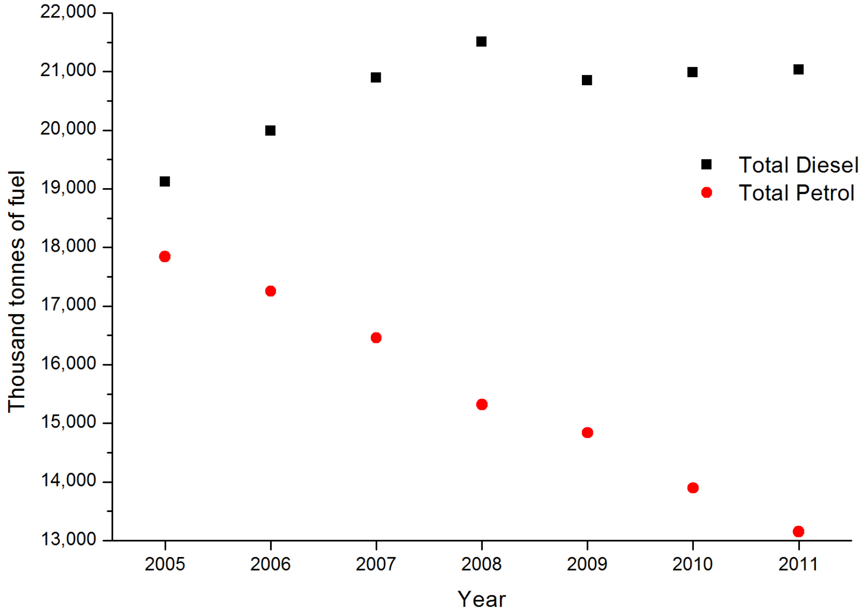

Figure 7. Change in fuel use from 2005 to 2011

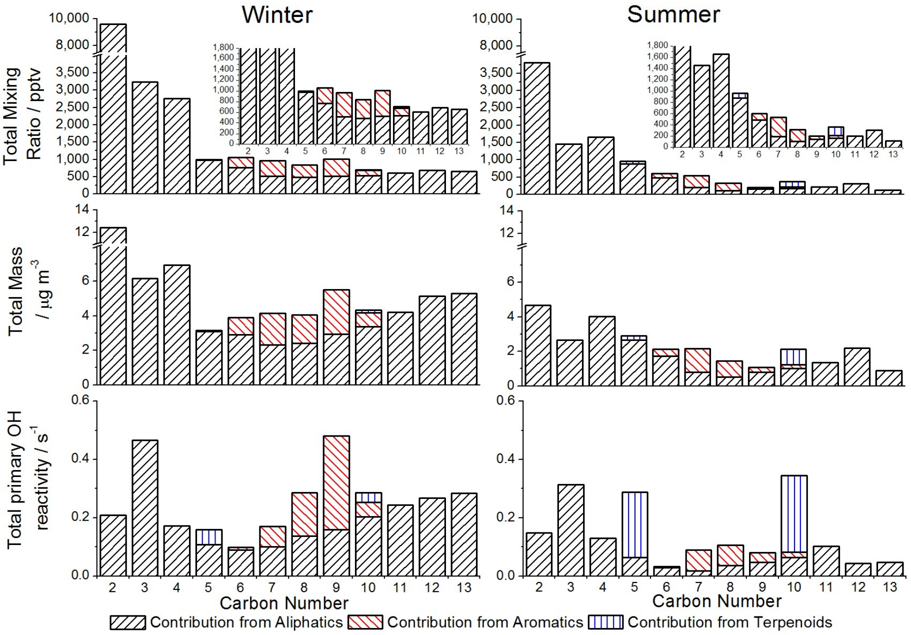

Figure 8. Seasonal median values for hydrocarbon mixing ratio, mass concentration and primary OH reactivity in London air grouped by carbon number and functionality

Table 1. Comparison of London, North Kensington, LA and Bakersfield

	Area (km^2)	Number of Inhabitants	Pop. density (inhab. km^{-2})	Cars per household	Percent public green space	Percent diesel use	Average Temp. (°C)		Average hrs sunlight	
							Winter	Summer	Winter	Summer
London	1572^a	7,825,200^a	4978^a	0.8^f	38.4^a	57^g	3^i	18.9^i	2.2k	5.9^k
NK	12.13^b	158,700^{c,d}	13,087^{c,d}	0.6^f		56^{c,g}				
LA	10510^a	9,818,605^a	934^a	1.9^3	6.7a	13^h	13.8^j	21.4^j	6.6^l	11.1^l
Bakersfield	244.77^b	357,603^3	1461^d			33^h				

References

[a] World Cities Cultural Report, 2013. [b] Calculated from Number of Inhabitants and Population density. [c] Values for Kensington and Chelsea. [d] Census, July 2012.
[e] US Census Bureau. [f] UK Office of National Statistics. [g] Department of Energy and Climate Change Statistics. [h] Gentner et al. (2012)
[i] metoffice.gov.uk, mean daily temperature. [j] los-angeles.climatemps.com/temperatures.php [k] metoffice.gov.uk, mean daily hours of sunshine.
[l] los-angeles.climatemps.com/sunlight.php

Table 2. Individually identified VOC mixing ratios, grouped by functionality, ordered by C number.

	Winter^a			Summer^b					
Compound	**Mean / pptv**	**Median / pptv**	**SD / pptv**	**Mean / pptv**	**Median / pptv**	**SD / pptv**	**LOD^c / pptv**	**Measured Using**	**Peak Identity^d**
Saturated									
Methane	2.24×10^6	2.18×10^6	3.45×10^5	1.83×10^6	1.81×10^6	1.44×10^5	100	DC-GC	-
Ethane	11,074	7,324	13,503	4,287	3,007	5,201	9	DC-GC	-
Propane	4,250	2,944	4,207	1,703	1,253	1,514	3	DC-GC	-
n-Butane	2,317	1,617	2,513	1,366	972	1,166	1	DC-GC	-
iso-Butane	1,359	916	1,424	686	473	624	1	DC-GC	-
n-Pentane	394	292	342	340	236	289	1	DC-GC	-
iso-Pentane	833	574	825	751	540	647	1	DC-GC	-
Cyclopentane	106	55	208	106	59	312	1	DC-GC	-
n-Hexane	122	85	112	91	60	82	1	DC-GC	7
Pentane, 2+3-methyl-	337	249	351	256	189	218	1	DC-GC	1
n-Heptane	89	62	99	66	49	57	1	DC-GC	16
Butane, 2,2,3-trimethyl-	111	78	107	71	55	50	1	GC×GC	12
n-Octane	32	22	101	21	16	18	2	DC-GC	24
Pentane, 2,2,4-trimethyl-	42	34	30	23	17	19	2	DC-GC	19
n-Nonane	526	380	481	128	102	99	3	GC×GC	28
n-Decane	398	328	339	132	87	138	2	GC×GC	41
Nonane, 2-methyl-	50	35	49	43	28	44	4	GC×GC	34
n-Undecane	397	288	364	165	125	123	1	GC×GC	50
n-Dodecane	374	321	279	273	207	244	1	GC×GC	51
Unsaturated									
Ethene	1,703	1,340	1,477	638	508	402	7	DC-GC	-
Acetylene	1,214	947	915	374	289	247	3	DC-GC	-
Propene	425	275	465	199	163	124	3	DC-GC	-
Propadiene	16	12	14	6	4	4	3	DC-GC	-
Propyne		N/a		44	37	16	3	DC-GC	-
Butene, *trans*-2-	43	29	44	20	16	14	1	DC-GC	-
1-Butene	75	53	68	61	53	31	1	DC-GC	-
iso-Butene	105	75	97	53	44	33	1	DC-GC	-
Butene, *cis*-2-	28	19	30	14	11	11	1	DC-GC	-
1,2-Butadiene		N/a		143	67	885	1	DC-GC	-
1,3-Butadiene	53	39	47	32	26	19	1	DC-GC	-
Pentene, *trans*-2-	48	29	152	26	21	24	1	DC-GC	-
1-Pentene	37	27	75	25	21	18	1	DC-GC	-
Isoprene	28	19	31	**117**	**88**	111	1	DC-GC	2
Styrene	34	17	54	33	19	34	8	GC×GC	30
α-Pinene	14	11	10	**94**	**77**	79	1	GC×GC	33
Limonene	4	2	7	**49**	**30**	52	3	GC×GC	44
Aromatics									
Benzene	356	293	236	147	117	93	2	DC-GC	15
Toluene	635	452	658	481	347	427	2	DC-GC	22
Benzene, ethyl-	140	99	118	81	61	70	3	DC-GC	26

[a] N/a indicates compounds that were not measured during the winter campaign
[b] Values in bold are higher during the summer campaign
[c] <LOD indicates values that are below the detection limit of the specified instrument, calculated at S/N = 3
[d] Peak identity corresponds to the labelled peaks in Figure 5

Table 2. continued.

Compound	Winter^a Mean / pptv	Winter^a Median / pptv	Winter^a SD / pptv	Summer^b Mean / pptv	Summer^b Median / pptv	Summer^b SD / pptv	LOD^c / pptv	Measured Using	Peak Identity^d
Aromatics continued									
m- and *p*-Xylene	185	128	181	113	81	104	3	DC-GC	27
o-Xylene	156	106	157	70	48	67	3	DC-GC	29
Benzene, *iso*-propyl-	27	21	22		<LOD		3	GC×GC	32
Benzene, propyl-	90	53	108	12	7	13	4	GC×GC	35
Toluene, 3-ethyl-	139	84	160	17	8	26	6	GC×GC	36
Toluene, 4-ethyl-	98	52	125	12	4	19	1	GC×GC	37
Benzene, 1,3,5-trimethyl-	93	64	90	12	7	16	5	GC×GC	38
Toluene, 2-ethyl-	65	41	71	8	3	12	6	GC×GC	39
Benzene, 1,2,4-trimethyl-	195	120	224	27	15	42	1	GC×GC	42
Toluene, 4-*iso*-propyl-	10	6	11	**35**	**24**	32	3	GC×GC	45
Benzene, 1,2,3-trimethyl-	66	42	76	7	3	10	1	GC×GC	46
Indan	11	8	9		<LOD		4	GC×GC	47
Benzene, *tert*-butyl-	7	4	7	10	3	14	1	GC×GC	43
Benzene, 1,3-diethyl-	6	3	6	7	4	9	2	GC×GC	48
Benzene, 1,4-diethyl-	5	3	7	3	2	3	1	GC×GC	49
Naphthalene	36	25	35	35	26	29	3	GC×GC	52
Oxygenates									
Acetaldehyde	2,256	1,703	1,680	**4,301**	**3,261**	3,207	1	DC-GC	-
Propanal, 2-methyl-		<LOD		**48**	**32**	43	6	GC×GC	5
Butanal	9	5	15	**13**	**8**	13	1	GC×GC	11
Butanal, 3-methyl-		<LOD		**28**	**19**	27	6	GC×GC	13
Butanal, 2-methyl-		<LOD		**21**	**12**	22	8	GC×GC	14
Methacrolein		<LOD		**24**	**15**	24	1	GC×GC	6
Pentanal		<LOD		**23**	**15**	21	8	GC×GC	18
Hexanal	9	6	10	**19**	**11**	19	3	GC×GC	25
Benzaldehyde	24	16	25	13	9	12	1	GC×GC	40
Methanol	1,246	962	1,605	**3,376**	**2,462**	2,580	40	DC-GC	-
Ethanol	5,005	3,514	4,557	4,978	3,506	4,229	9	DC-GC	-
Propanol	370	209	699	252	183	195	10	DC-GC	-
Butanol	1,157	748	1,538	484	376	488	20	DC-GC	-
Acetone	1,076	896	565	**2,405**	**2,114**	1,093	9	DC-GC	3
Butanone	29	25	22	**64**	**44**	54	2	GC×GC	10
Ketone, methyl-vinyl-		<LOD		**33**	**22**	32	4	GC×GC	8
Pentanone, 2-		<LOD		**29**	**19**	28	1	GC×GC	17
Pentanone, 4-methyl-2-	36	10	57	**51**	**33**	48	1	GC×GC	21
Hexanone, 2-		<LOD		**38**	**27**	33	3	GC×GC	23
Cyclohexanone		<LOD		**17**	**11**	18	9	GC×GC	31
Acetate, ethyl-	45	34	40	46	30	44	2	GC×GC	9
Halogenated									
Methane, dichloro	29	18	31	**35**	**25**	29	2	GC×GC	4
Trichloroethylene		<LOD		**10**	**7**	8	5	GC×GC	20

[a] N/a indicates compounds that were not measured during the winter campaign

[b] Values in bold are higher during the summer campaign

[c] <LOD indicates values that are below the detection limit of the specified instrument, calculated at S/N = 3

[d] Peak identity corresponds to the labelled peaks in Figure 5

Table 3. Grouped VOC mixing ratio and the number of isomers in each group.

Groups	Number of Isomers^a	Winter^b Mean / pptv	Winter^b Median / pptv	Winter^b SD / pptv	Summer^{b,c} Mean / pptv	Summer^{b,c} Median / pptv	Summer^{b,c} SD / pptv
C_6 Aliphatics	9	502	434	256	304	234	250
C_7 Aliphatics	10	586	379	617	127	93	132
C_8 Aliphatics	25	602	427	572	107	78	106
C_9 Aliphatics	28	214	143	220	79	49	98
C_{10} Aliphatics	40	283	176	340	95	61	147
C_{11} Aliphatics	41	459	320	452	137	89	209
C_{12} Aliphatics	37	591	363	696	163	111	244
C_{13} Aliphatics	30	937	654	914	187	117	170
C_4 substituted monoaromatics	16	210	102	298	33	14	57
C_{10} Monoterpenes	25	13	7	17	**51**	**34**	48

[a] The number of isomers correspond to the groupings shown in the GC×GC-FID plot shown in Figure 2 of the main paper

[b] Cumulative mixing ratio of each specified compound group not including those given individually in Table 2
(*i.e.* the C_7 aliphatics are not including *n*-Heptane and 2,2,3-trimethyl butane)

[c] Values in bold are higher during summer campaigns

Table 4. Room Temperature Rate Constants for the Gas-Phase Reactions of OH Radicals with C_{12} Aliphatic Compounds (Atkinson, 2003; Ziemann and Atkinson, 2012; Kwok and Atkinson, 1995; Atkinson and Arey, 2003; Aschmann and Atkinson, 2008).

		$10^{12} \times k_{OH}{}^{a}$ (cm^3 molecules^{-1} s^{-1})	
Species	**Structure**	**Measured**[b]	**Calculated**[c]
Alkanes (linear, branched, cyclic)			
n-dodecane	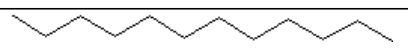	13.2[d]	13.9
2-methylundecane		-	13.9
2,2-dimethyldecane	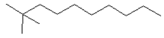	-	10.3
3,3,4-trimethylnonane	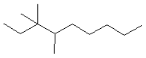	-	8.79
6-ethyl-3-methylnonane	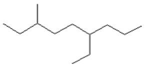	-	14.9
2,2,3,3,4,4-hexamethylhexane	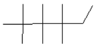	-	2.49
cyclododecane	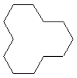	-	17.0
Alkenes/dienes			
1-dodecene	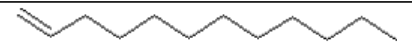	50.3±1.3[e]	47.1
trans-5-dodecene	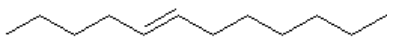	-	71.1
2,9-dimethyl-1,9-decadiene	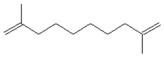	-	77.8
2,4-dimethyl-2,4-decadiene	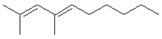	-	176

[a] All data measured/calculated at atmospheric pressure.
[b] 298 K data taken from Atkinson (2003) unless otherwise stated; estimated uncertainty of ± 20 % unless otherwise stated.
[c] Calculated using the hydroxyl radical H-atom abstraction and OH addition structure activity relationships given in Ziemann and Atkinson (2012) and Kwok and Atkinson (1995) respectively; calculated rate constants for alkanes and alkenes within a factor of 2 of those measured.
[d] Atkinson and Arey (2003)
[e] 295 ± 1 K relative rate data taken from Aschmann and Atkinson (2008).

Table 5. Primary hydrocarbon OH reactivity (s^{-1}) divided by emission source for winter and summer

	Natural Gas	**Gasoline**	**Total Diesel (Measured + Calculated (±error))**	**Biogenic**	**OVOCs**	**Total (±error)**
Winter	0.51	1.73	5.13 (1.02 + 4.10 (±0.51))	0.03	1.23	8.64 (±0.51)
Summer	0.27	0.77	1.72 (0.30 + 1.42 (±0.18))	0.50	1.74	5.00 (±0.18)

Table 6. Contribution of total diesel to mixing ratio, mass, primary hydrocarbon OH reactivity and ozone formation potentials with and without C_9 aromatic species

	Winter		Summer	
	With C_9 aromatics	Without C_9 aromatics	With C_9 aromatics	Without C_9 aromatics
Mixing Ratio / %	34.5 ± 3.5	34.2 ± 3.5	21.2 ± 2.2	21.1 ± 2.2
Mass / %	63.5 ± 6.5	63.0 ± 6.5	46.3 ± 4.8	46.2 ± 4.8
OH reactivity / %	59.3 ± 5.9	58.3 ± 5.9	34.4 ± 3.6	34.2 ± 3.6
Ozone formation potential / %	45.6 ± 4.6	43.5 ± 4.6	26.3 ± 4.8	25.9 ± 4.8

Table 7. Fuel use changes for the UK

	Personal Vehicles				Freight					%
Year	**Buses**	**Diesel Cars**	**Petrol Cars**	**Motor Cycles**	**HGV**	**Diesel LGV**	**Petrol LGV**	**Total Diesel**[a]	**Total Petrol**[b]	**Diesel Use**[c]
2005	1,453.0	5,836.0	17,267.0	198.0	7,577.0	4,250.0	377.0	19,116.0	17,842.0	52
2006	1,476.0	6,314.0	16,687.0	188.0	7,778.0	4,424.0	378.0	19,992.0	17,253.0	54
2007	1,552.0	6,731.0	15,913.0	200.0	7,956.0	4,651.0	345.0	20,890.0	16,458.0	56
2008	1,505.0	7,295.0	14,830.0	183.0	8,054.0	4,652.0	306.0	21,506.0	15,319.0	58
2009	1,501.0	7,370.0	14,373.0	187.0	7,413.0	4,561.0	277.0	20,845.0	14,837.0	58
2010	1,495.0	7,375.0	13,477.0	166.0	7,511.0	4,606.0	252.0	20,987.0	13,895.0	60
2011	1,383.0	7,663.0	12,750.0	167.0	7,311.0	4,678.0	234.0	21,035.0	13,151.0	62

[a] Total Diesel calculated as the sum of buses, diesel cars, HGV and diesel LGV

[b] Total Petrol calculated as the sum of petrol cars, motorcycles and petrol LGV

[c] % diesel use calculated as (total diesel divided by total fuel (sum total diesel and petrol)) x 100